Available online at www.sciencedirect.com

SciVerse ScienceDirect

Ceramics International 38 (2012) 5661–5667

CERAMICS INTERNATIONAL

www.elsevier.com/locate/ceramint

The influence of B_4C and MgB_2 additions on the behavior of MgO–C bricks

Karina S. Campos [a,1], Guilherme F.B. Lenz e Silva [b], Eduardo H.M. Nunes [a,*], Wander L. Vasconcelos [a,2]

[a] Federal University of Minas Gerais, Dept. of Metallurgical and Materials Engineering, Laboratory of Ceramic Materials, Avenida Presidente Antônio Carlos, 6627 – sala 2230 Pampulha, Campus UFMG – Escola de Engenharia, bloco 2, CEP 31270-901, Belo Horizonte, MG, Brazil

[b] University of São Paulo, Dept. of Metallurgical and Materials Engineering, Avenida Mello Moraes, 2463 – sala 4 – Cidade Universitária, CEP 05508-030, São Paulo, SP, Brazil

Received 23 August 2011; received in revised form 13 February 2012; accepted 3 April 2012
Available online 12 April 2012

Abstract

Carbon-containing refractory materials have received great attention over the last years due to their importance in the steelmaking process. The oxidation of carbon present in refractory materials at temperatures above 500 °C is usually accompanied by the decrease of their mechanical strength and chemical resistance. Aiming to improve the oxidation resistance of carbon-oxide refractories, the use of materials known as antioxidants has been extensively studied. In this work we evaluated the performance of MgB_2 and B_4C antioxidants when incorporated into MgO–C bricks. We observed that the co-addition of metallic antioxidants and B_4C or MgB_2 leads to refractory bricks with enhanced hot modulus of rupture and resistance against oxidation and slag corrosion. However, the excessive addition of these antioxidants could impair the performance of the obtained bricks. Thus, when determining the optimum concentration of MgB_2 and B_4C to be added into MgO–C refractories, one must take into consideration this behavior.

Keywords: C. Corrosion; C. Strength; D. Carbon; D. MgO

1. Introduction

Magnesia carbon refractories have been widely used in slag line of steel ladles, BOF/LD (Basic Oxygen Furnaces/Linz Donawitz) converters, and electric arc furnaces (EAF). They usually show great resistance against chemical attack from slag and thermal shock. It is well established that this behavior arises from the presence of carbon in these materials [1,2]. Due to the low concentration of residual carbon in ungraphitized carbon and its low oxidation resistance, flake graphite has been the major carbon source for the refractory industry. It is stated in the literature that flake graphite improves some properties of refractory materials, including their resistance against thermal shock and chemical attack, thermal conductivity, and fracture toughness [3,4].

The oxidation of carbon present in refractory materials at temperatures above 500 °C is usually accompanied by the decrease of their mechanical strength and chemical resistance. This behavior arises from the increase of the refractory porosity [5–9]. In order to improve the oxidation resistance of oxide-carbon refractories, the use of materials known as antioxidants has been extensively studied. Metal-powders and their alloys improve the mechanical strength and oxidation resistance of carbon-containing refractory materials. Boron-based non-oxide ceramics also have shown successful results [10]. Antioxidant materials easily react with oxygen and carbon, leading to the blocking of pores and mitigating carbon oxidation by the formation of liquid phases [11,12]. The appropriate selection of the antioxidant to be used (type and amount) in a given application will depend on several parameters, including the refractory composition, heat treatment conditions (atmosphere and target temperature), slag chemical composition, and thermomechanical stresses that develop during the process.

In this work we evaluated the performance of MgB_2 and B_4C antioxidants when incorporated into MgO–C bricks. We also evaluated the bulk density, apparent porosity, three-point bending strength, and cold crushing strength (CCS) of brick

* Corresponding author.
E-mail addresses: karinaespanhol@hotmail.com (K.S. Campos), eduardohmn@yahoo.com.br (E.H.M. Nunes), wlv@demet.ufmg.br (W.L. Vasconcelos).
[1] Tel.: +55 31 3409 1813.
[2] Tel.: +55 31 3409 1821.

0272-8842/$36.00
http://dx.doi.org/10.1016/j.ceramint.2012.04.009

samples after drying at 200 °C. Properties such as the oxidation and corrosion behavior of these materials, as well as their hot modulus of rupture (HMOR) were investigated. After performing oxidation tests, we observed by X-ray diffraction (XRD) the crystalline phases formed in both oxidized and non-oxidized portions of the composites. Ceramographic examinations were carried out by reflected light and scanning electron microscopies (LM and SEM, respectively).

2. Materials and methods

Electrofused magnesia (4.75 mm – <600 μm – from Magnesita SA), MgO sinter (<212 μm – from Magnesita SA), flake graphite (∼180 μm – from Nacional de Grafite), and liquid phenolic resin (2.60 wt% – from Dynea) were used in the processing of MgO–C refractory bricks. Previous tests revealed that flake graphite has chemical purity of ca. 99%. Table 1 gives the chemical composition of electrofused magnesia and MgO sinter. Table 2 gives the antioxidants added into the prepared MgO–C bricks. It is important mentioning that A1 is a reference formulation, typically used in oxygen converters. The antioxidants used in this study present mean particle sizes below 45 μm.

A typical processing procedure used in this study is as follows: first, a ceramic mass was obtained by mixing electrofused magnesia, MgO sinter, flake graphite, and the antioxidant related to each composition (see Table 2). Next, the obtained ceramic mixture was homogenized in an intensive mixer. Lastly, liquid phenolic resin was slowly added in order to act as a binder in the obtained materials. The forming of MgO–C bricks was carried out using a friction press. Samples were obtained in suitable size and shape to perform the mechanical (HMOR/bending strength – 160 mm × 40 mm × 40 mm, CCS – 80 mm × 40 mm × 40 mm), oxidation (40 mm × 40 mm × 40 mm), and corrosion tests (160 mm × 70 mm × 40 mm). Curing of samples was carried out in air at room temperature for 24 h. In order to dry the MgO–C bricks, they were kept at 200 °C for 6 h.

Table 1
Chemical composition of electrofused magnesia and MgO sinter used in this work.

Composition	Concentration (wt%)	
	Electrofused magnesia	MgO sinter
MgO	97.85	98.40
CaO	0.94	0.77
SiO_2	0.43	0.25
Al_2O_3	0.22	0.05
Fe_2O_3	0.42	0.41
MnO	0.07	0.12
B_2O_3	ND	0.007
Cr_2O_3	0.07	ND

ND: Not detected.

Table 2
Antioxidants added into the prepared MgO–C bricks.

Antioxidant	Manufacturer	Composition (wt%)			
		A1	A2	A3	A4
Coated aluminum powder	Alcoa	1–3	–	1–3	1–3
Mg–Al alloy (50:50)	ACCR Trading Company	1–3	–	1–3	1–3
MgB_2	Sigma–Aldrich	–	–	0.25	–
B_4C	Washington Mills	–	–	–	0.25

The bulk density and apparent porosity of samples dried at 200 °C was evaluated by the Archimedes immersion technique and as described in the Brazilian standard (NBR 6220). XRD analyses were carried out in a PANalytical X' Pert Pro diffractometer, using Cu Kα radiation. XRD patterns were recorded in the angle range from 5° to 65° (2θ), at a scan velocity of 0.127°/s. The identification of crystalline phases was performed using JCPDS files numbers 12-0212, 21-1152, 25-0161, 35-0799, and 45-0946 for graphite, $MgAl_2O_4$, $Ca_3Mg_2(SiO_4)_2$, Al_4C_3, and MgO, respectively. SEM analyses were performed in a JEOL JSM-6360 LV scanning electron microscope. Compositional analyses were carried out using a NORAN EDS system available in the SEM equipment. Samples were prepared for LM investigations by embedding them in epoxy resin, followed by grinding and polishing until diamond paste of 1 μm grain size.

Bending strength and CCS tests were carried out at room temperature, using a Kratos press (model ECC 100MP) and according to the Brazilian standard (ABNT NBR 6113/ABNT NBR 6224). HMOR tests were performed at 900 °C, 1200 °C, and 1400 °C, using a heating rate of 140 °C/h and keeping samples at the target temperature for 30 min. These tests were carried out using a MTS press (model 318.25) and as described in ASTM C583-10 procedure. Samples used in these tests were enclosed in a nickel foil to prevent their superficial oxidation. Oxidation tests were carried out at 1400 °C, keeping samples at this temperature for 1 h. During oxidation tests there was a continuous injection of compressed air in order to obtain an oxidizing atmosphere. Slag corrosion tests were performed in an induction furnace, using a heating rate of 26 °C/min. A typical slag from a LD converter and steel samples were added in the furnace until the temperature of 1600 °C was reached. At each 30 min interval the slag was renewed in order to maintain its reactivity during the test. The duration of each corrosion test was about 3 h. A typical chemical composition of the slag used in these tests is the following: CaO/SiO_2 (>2.5%), Fe (≈20.0 wt%), and MgO (7.0 wt%). Slag corrosion tests were performed as described in ASTM C874-99 standard. It is important mentioning that bending strength, CCS, HMOR, corrosion, and oxidation tests were carried out in samples after the drying step (200 °C).

3. Results and discussion

3.1. Morphological and XRD results

Fig. 1 shows a typical LM micrograph of an antioxidant-containing MgO–C brick after drying at 200 °C. One observes among MgO grains (dark gray) the refractory matrix mainly composed by graphite (light gray), MgO fines, and antioxidant

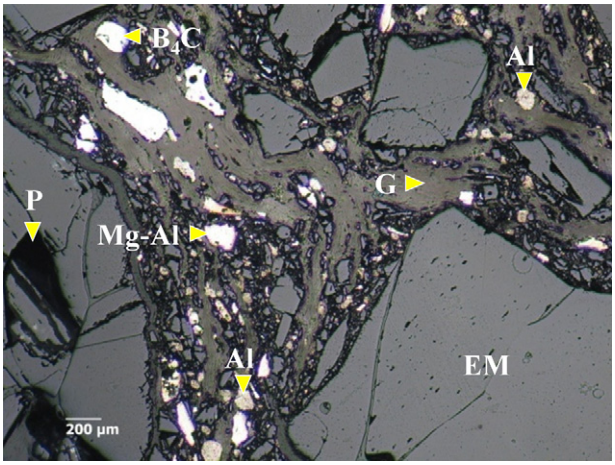

Fig. 1. Typical LM micrograph of an antioxidant-containing MgO–C brick after drying at 200 °C. The scale bar corresponds to 200 µm.

particles. Fig. 2 depicts XRD patterns of oxidized and non-oxidized portions of samples used in oxidation tests.

Fig. 3 exhibits SEM micrographs of MgO–C bricks prepared in this work. The micrographs of non-oxidized areas revealed the presence of spheroidal phase of aluminum carbide (Al_4C_3) dispersed in the refractory matrix. We believe that these particles are present in sites previously occupied by metallic aluminum. Some of the micrographs shown in Fig. 3 reveal the presence of MgO grains enclosing aggregates of Al_4C_3 particles. These aggregates usually present Al and Ca particles in their frameworks. We also believe that these particles could arise from impurities present in electrofused magnesia particles (see Fig. 3I, II, V, VI, VII and VIII). XRD and EDS tests revealed that spinel ($MgAl_2O_4$) is initially formed in these areas. We observed that $MgAl_2O_4$ is present in greater concentrations in oxidized areas than in non-oxidized ones. Merwinite ($Ca_3Mg(SiO_4)_2$) was occasionally observed in MgO grain boundaries (see Fig. 3I–IV). We did not observe the presence of $Ca_3Mg(SiO_4)_2$ in micrographs shown in Fig. 3VII and VIII.

It is well established that the detection limit of EDS and XRD is about 0.5 wt% and 5 wt%, respectively [13–17]. Since MgB_2 and B_4C were added into MgO–C bricks in a concentration of 0.25 wt%, it was not possible to observe the presence of these antioxidants by these techniques.

3.2. Bulk density, apparent porosity, bending strength, and CCS tests

Fig. 4 shows the bulk density and apparent porosity of refractory bricks prepared in this work. We observed that all samples exhibited green densities of about 3.0 g/cm^3. On the other hand, A2 showed the greater porosity among the tested formulations. Fig. 5 depicts the MOR and CCS of these samples. One notices that these materials presented similar MOR and CCS. This behavior suggests that the drying temperature of 200 °C is not sufficient to cause remarkable microstructural changes in the prepared bricks. Such microstructural changes are more pronounced only after the firing step, typically performed at temperatures above 1000 °C.

3.3. HMOR tests

Fig. 6 shows the HMOR of bricks prepared in this work. One observes that the co-addition of boron-based antioxidants and Mg–Al alloy leads to samples with enhanced HMOR (see A3 and A4). We believe that both the added boron-based antioxidant and aluminum carbide (formed by the reaction of Mg–Al alloy with carbon atoms from the brick) play an important role in this process. However, the addition of high contents of boron-based antioxidants into MgO–C bricks could lead to decreasing their mechanical strength. This behavior is due to the occurrence of the following reaction [18]:

$$3MgO_{(s)} + B_2O_{3(l)} \rightleftharpoons 3MgO \cdot B_2O_3 \quad (1)$$

where $B_2O_{3(l)}$ is a product of boron carbide oxidation and $MgO_{(s)}$ could arise from magnesia sinter or electrofused magnesia. It is well established that the presence of $3MgO{\cdot}B_2O_{3(l)}$ decreases the refractoriness, slag resistance, and HMOR of the brick.

One would expect that the presence of $Ca_3Mg(SiO_4)_2$ and $3MgO{\cdot}B_2O_3$ in the obtained MgO–C bricks could impair their HMOR. However, these phases are present in such low concentration in these materials that they do not decrease the mechanical strength of the refractory bricks.

3.4. Oxidation tests

Fig. 7 depicts the oxidation resistance of refractory bricks obtained in this study. One notices that A2 exhibited the lower oxidation resistance among the analyzed samples. Moreover, the co-addition of metallic antioxidants and MgB_2 or B_4C leads to bricks with enhanced oxidation resistance (see A3 and A4). The combined use of MgB_2 and metallic antioxidants leads to the formation of an oxide layer on the refractory surface consisting of $MgAl_2O_3$, MgO, and a glassy boron-oxide layer. According to Ichikawa et al. [19], this oxide layer act as a barrier to oxygen diffusion. However, its protective effect against oxidation is impaired at temperatures above 1000 °C [19]. We believe that the distinct oxidation behavior of A3 and A4 could be ascribed to the formation of $3MgO{\cdot}B_2O_3$ in the framework of A4 (see Eq. (1)). Palco et al. [20] reported that $3MgO{\cdot}B_2O_3$ can inhibit the oxygen diffusion into the refractory.

3.5. Slag corrosion tests

Fig. 8(a) depicts the percent wear of MgO–C bricks used in slag corrosion tests. Fig. 8(b) shows the corrosion profile of these samples. In general, all samples exhibited a good resistance against slag attack. We observed that A4 showed the higher resistance followed by A3, A1, and A2. However, one notices that there is a little difference among the corrosion

behavior of these samples. It is well established that there is an optimum concentration of these antioxidants in which it is possible to inhibit the carbon oxidation without impair the corrosion resistance of the refractory. As mentioned before, non-metallic antioxidant easily react with oxygen and carbon, leading to the blocking of pores by the formation of liquid phases. In addition, metallic antioxidants lead to the formation of an oxide layer at the slag–refractory interface [20]. Lee and Zhang

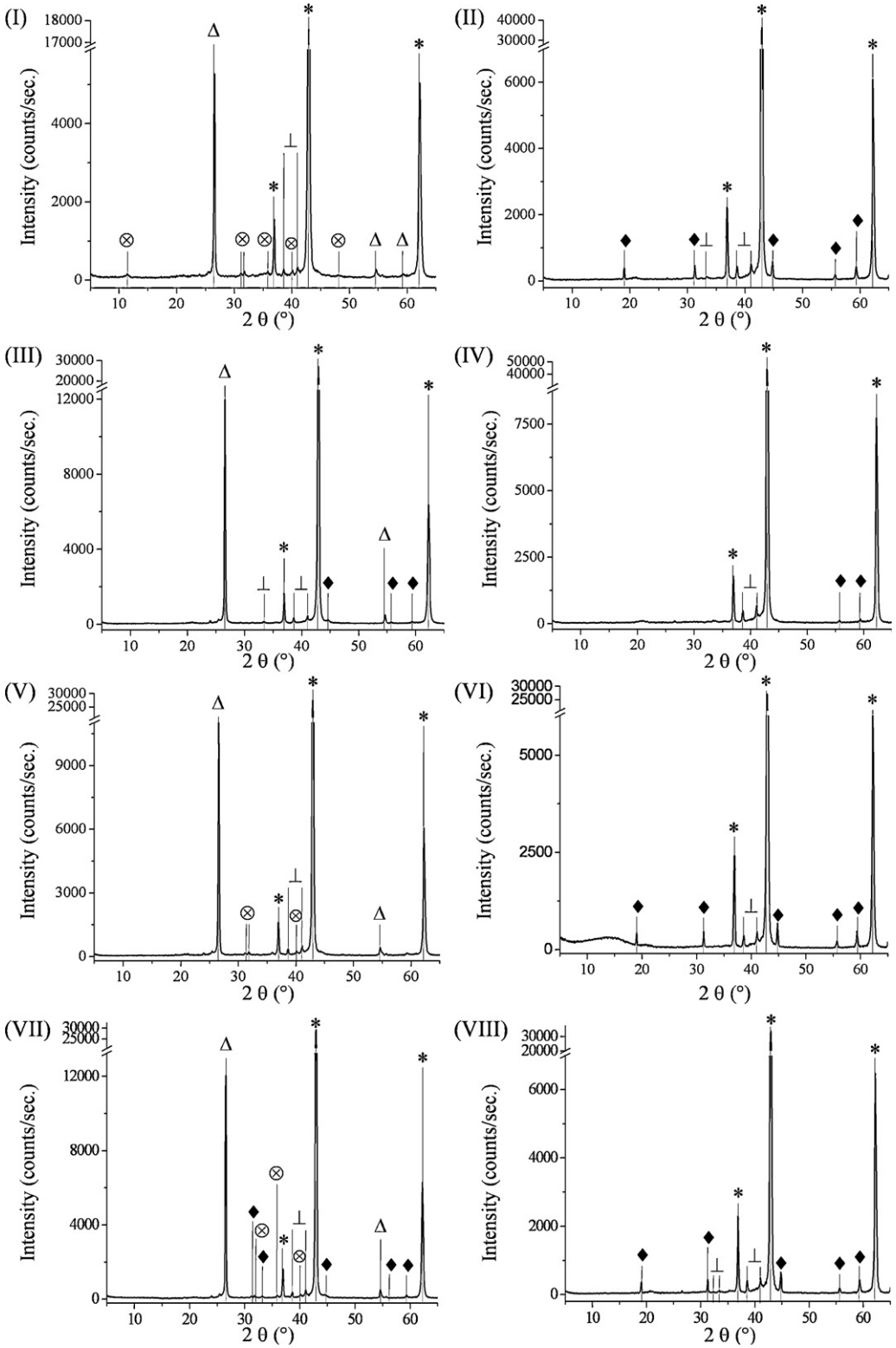

Fig. 2. XRD patterns of samples used in oxidation tests. (I), (III), (V), and (VII) represent non-oxidized portions of A1, A2, A3, and A4, respectively. (II), (IV), (VI), and (VIII) represent oxidized portions of A1, A2, A3, and A4. * MgO/Δ Graphite/⊗ Al_4C_3/⊥ $Ca_3Mg(SiO_4)_2$/◆ $MgAl_2O_4$.

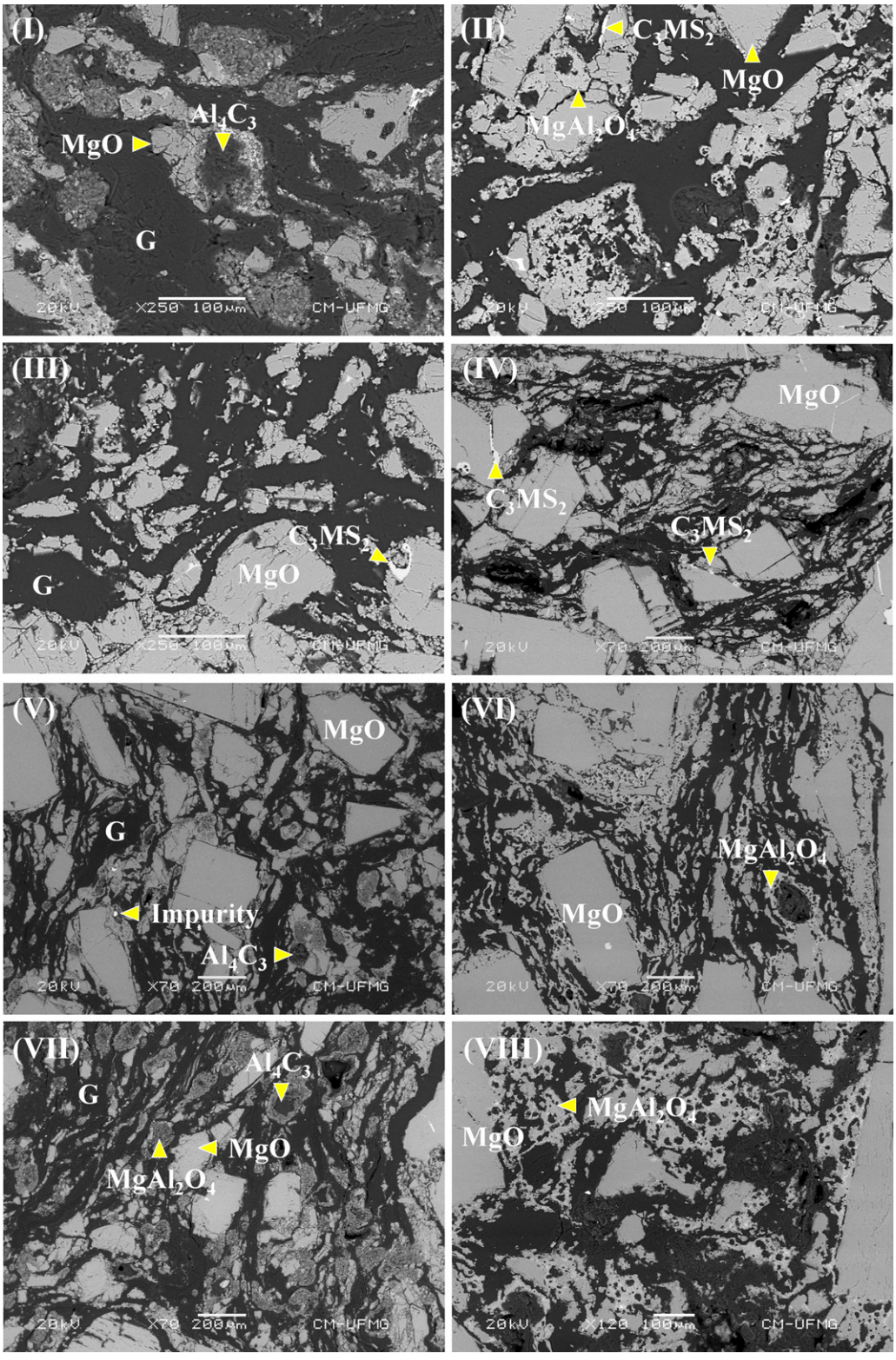

Fig. 3. SEM micrographs of non-oxidized and oxidized areas of MgO–C bricks used in oxidation tests. (I and II) Al + Mg–Al alloy; (III and IV) In natura (without antioxidant); (V and VI) Al + Mg–Al alloy + MgB_2; (VII and VIII) Al + Mg–Al alloy + B_4C. C_3MS_2: $Ca_3Mg(SiO_4)_2$. The scale bars correspond to 100 μm in (I), (II), (III), and (VIII), and to 200 μm in (IV), (V), (VI), and (VII).

[21] reported that this oxide layer can also be formed in the brick framework. The reason why B_4C-containing refractory (A4) showed a higher resistance than MgB_2-containing one (A3) is not fully understood due, in great part, to the lack of thermodynamic data about boron-containing non-oxide ceramics. Thus, further investigations are needed to understand the effect of adding MgB_2 on the resistance against slag attack of magnesia carbon refractories.

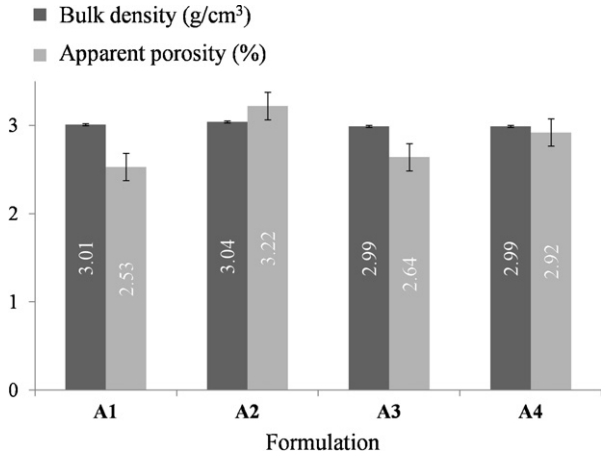

Fig. 4. Bulk density and apparent porosity of refractory bricks prepared in this work.

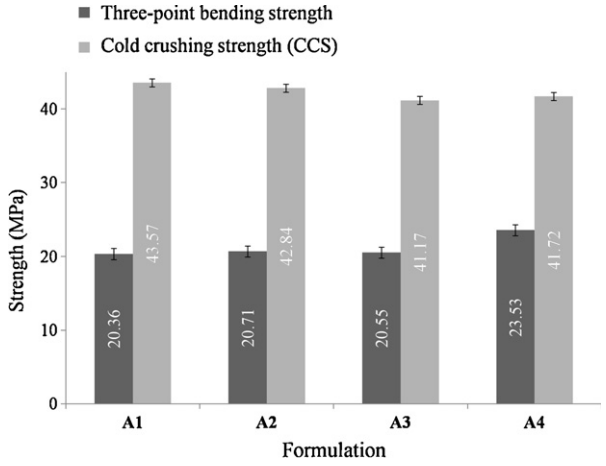

Fig. 5. Bending strength and CCS of refractory bricks obtained in this work.

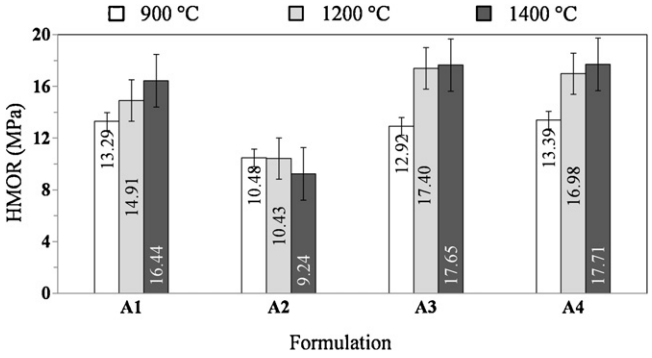

Fig. 6. HMOR of bricks prepared in this work.

4. Conclusions

We observed that the prepared bricks exhibited green densities of about 3.0 g/cm^3. A2 showed the greater porosity among the tested formulations. All tested materials showed similar bending strength and CCS. We also observed that the co-addition of metallic antioxidants and B_4C or MgB_2 leads to refractory bricks with enhanced hot modulus of rupture and resistance against oxidation and slag corrosion. However, the excessive addition of these antioxidants could impair the performance of the obtained bricks. Thus, when determining the optimum concentration of MgB_2 and B_4C to be added into MgO–C refractories, one must take into consideration this behavior.

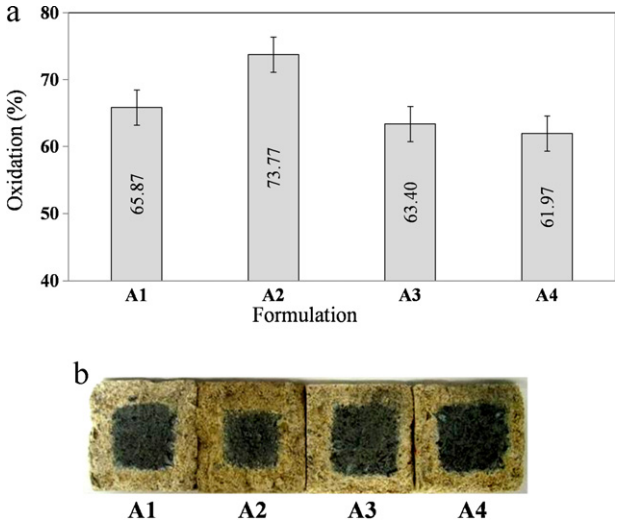

Fig. 7. Oxidation resistance of refractory bricks obtained in this study.

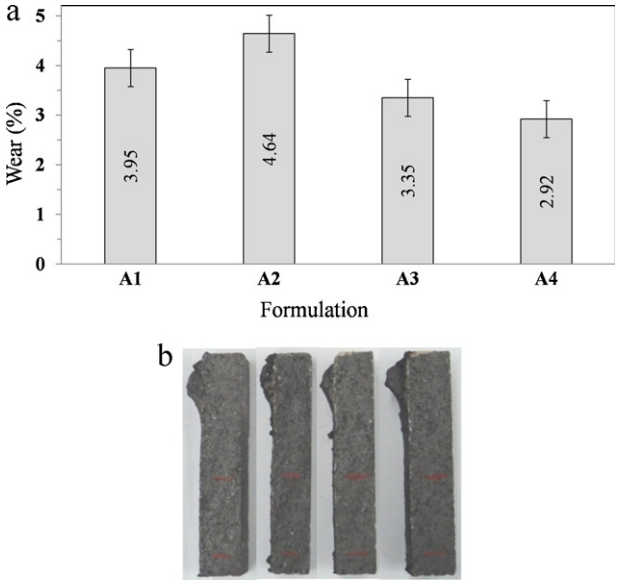

Fig. 8. (a) Percent wear of MgO–C bricks used in slag corrosion tests. (b) Corrosion profile of these samples.

Acknowledgments

The authors thank Magnesita S.A. and CAPES/FAPEMIG for the technical and financial support to this research, respectively.

References

[1] A.S. Gokce, C. Gurcam, S. Ozgen, S. Aydin, The effect of antioxidants on the oxidation behavior of magnesia-carbon refractory bricks, Ceramics International 34 (2008) 323–330.

[2] J.A. Rodrigues, V.C. Pandolfelli, R-curve behavior of MgO–C refractories (comportamento de curva-R de refratários de MgO–C), Ceramics 46 (2000) 40–47 (in portuguese).

[3] P.O.R.C. Brant, V.C. Cruz, Brazilian flake graphites for carbon containing refractories, in: Proc. Unif. Int. Tech. Conf. Refract. (UNITECR), São Paulo, Brazil, 1993.

[4] S. Zhang, W.E. Lee, Carbon containing castables: current status and future prospects, British Ceramic Transactions 101 (2002) 1–8.

[5] T. Wang, A. Yamaguchi, Oxidation protection of MgO–C refractories by means of Al8B4C7, Journal of the American Ceramic Society 84 (2001) 577–582.

[6] S.K. Sadrnezhaad, Z.A. Nemati, S. Mahshid, S. Hosseini, B. Hashemi, Effect of Al antioxidant on the rate of oxidation of carbon in MgO–C refractory, Journal of the American Ceramic Society 90 (2007) 509–515.

[7] S. Zhanga, N.J. Marriotta, W.E. Lee, Thermochemistry and microstructures of MgO–C refractories containing various antioxidants, Journal of the American Ceramic Society 21 (2001) 1037–1047.

[8] V.G. Domiciano, Carbon-rich refractory concretes [concretos refratários contendo elevado teor de carbono], M.Sc. Dissertation, Federal University of São Carlos, São Carlos, 2005 (in portuguese).

[9] M. Chen, N. Wang, J. Yu, A. Yamaguchi, Oxidation protection of CaO–ZrO_2–C refractories by addition of SiC, Ceramics International 33 (2007) 1585–1589.

[10] E.M.H. Ewais, Carbon-based refractories, Journal of the Ceramic Society of Japan 112 (2004) 517–532.

[11] A.P. Luz, New refractory concretes with high content of carbon [concretos refratários avançados com alto teor de carbono], Ph.D. Thesis, Federal of São Carlos, São Carlos, 2010 (in portuguese).

[12] V.G. Domiciano, J.R. Garcia, V.C. Pandolfelli, Water corrosion resistance of metal powders for carbon containing castables, American Ceramic Society Bulletin 86 (2007) 9401–9406.

[13] B. Dold, Speciation of the most soluble phases in a sequential extraction procedure adapted for geochemical studies of copper sulfide mine waste, Journal of Geochemical Exploration 80 (2003) 55–68.

[14] K. Kukkadapu, J.M. Zachara, J.K. Fredrickson, S.C. Smith, A.C. Dohnalkova, C.K. Russell, Transformation of 2-line ferrihydrite to 6-line ferrihydrite under oxic and anoxic conditions, American Mineralogist 88 (2003) 1903–1914.

[15] W. Yang, S.S. Hullavarad, B. Nagaraj, I. Takeuchi, R.P. Sharma, T. Venkatesan, R.D. Vispute, H. Shen, Compositionally tuned epitaxial cubic $Mg_xZn_{1-x}O$ on Si(100) for deep ultraviolet photodetectors, Applied Physics Letters 82 (2003) 3424–3426.

[16] D.Y. Jiang, J.Y. Zhang, K.W. Liu, Y.M. Zhao, C.X. Cong, Y.M. Lu, B. Yao, Z.Z. Zhang, D.Z. Shen, A high-speed photoconductive UV detector based on an $Mg_{0.4}Zn_{0.6}O$ thin film, Semiconductor Science and Technology 22 (2007) 687–690.

[17] D.Y. Jiang, D.Z. Shen, K.W. Liu, C.X. Shan, Y.M. Zhao, T. Yang, B. Yao, Y.M. Lu, J.Y. Zhang, Effect of post annealing on the band gap of $Mg_xZn_{1-x}O$ thin films, Semiconductor Science and Technology 23 (2008) 1–5.

[18] M. Rigaud, New additives in carbon-bonded refractories, in: Advances in Science and Technology Ceramics – Charting the Future, 1995 pp.399–413.

[19] K. Ichikawa, N. Tsukamoto, O. Nomura, N. Imai, Effects of Mg-B material addition to Al_2O_3–C SV plate, Taikabutsu Overseas 15 (1995) 33–37.

[20] S. Palco, L. Xiangmin, M. Rigaud, Synergetic effects of boron-based antioxidant combined with aluminium additive in magnesia–carbon refractories, Journal of the Canadian Ceramic Society 63 (1994) 261–265.

[21] W.E. Lee, S. Zhang, Direct and indirect slag corrosion of oxide and oxide-c refractories, in: VII International Conference on Molten Slags Fluxes and Salts, 2004, 309–319.